Mechanism of the Voltage Sensitivity of IRK1 Inward-rectifier K^+ Channel Block by the Polyamine Spermine

Hyeon-Gyu Shin and Zhe Lu

Department of Physiology, University of Pennsylvania, Philadelphia, PA 19104

ABSTRACT IRK1 (Kir2.1) inward-rectifier K^+ channels exhibit exceedingly steep rectification, which reflects strong voltage dependence of channel block by intracellular cations such as the polyamine spermine. On the basis of studies of IRK1 block by various amine blockers, it was proposed that the observed voltage dependence (valence ~5) of IRK1 block by spermine results primarily from K^+ ions, not spermine itself, traversing the transmembrane electrical field that drops mostly across the narrow ion selectivity filter, as spermine and K^+ ions displace one another during channel block and unblock. If indeed spermine itself only rarely penetrates deep into the ion selectivity filter, then a long blocker with head groups much wider than the selectivity filter should exhibit comparably strong voltage dependence. We confirm here that channel block by two molecules of comparable length, decane-*bis*-trimethylammonium (bis-QA_{C10}) and spermine, exhibit practically identical overall voltage dependence even though the head groups of the former are much wider (~6 Å) than the ion selectivity filter (~3 Å). For both blockers, the overall equilibrium dissociation constant differs from the ratio of apparent rate constants of channel unblock and block. Also, although steady-state IRK1 block by both cations is strongly voltage dependent, their apparent channel-blocking rate constant exhibits minimal voltage dependence, which suggests that the pore becomes blocked as soon as the blocker encounters the innermost K^+ ion. These findings strongly suggest the existence of at least two (potentially identifiable) sequentially related blocked states with increasing numbers of K^+ ions displaced. Consequently, the steady-state voltage dependence of IRK1 block by spermine or bis-QA_{C10} should increase with membrane depolarization, a prediction indeed observed. Further kinetic analysis identifies two blocked states, and shows that most of the observed steady-state voltage dependence is associated with the transition between blocked states, consistent with the view that the mutual displacement of blocker and K^+ ions must occur mainly as the blocker travels along the long inner pore.

KEY WORDS: Kir • energetics • kinetics • valence • quaternary ammonium

INTRODUCTION

Inward-rectifier K^+ (Kir) channels accomplish numerous important biological tasks because of their ability to conduct K^+ current in an inwardly rectifying manner (Katz, 1949; Hodgkin and Horowicz, 1959; Noble, 1962, 1965; Hagiwara and Takahashi, 1974; Hagiwara et al., 1976; Ashcroft, 2000; Hille, 2001; Stanfield et al., 2002). The exceedingly steep rectification in IRK1 (Kir2.1) channels reflects a strong voltage dependence of pore block by long intracellular polyamines such as spermine (Ficker et al., 1994; Lopatin et al., 1994; Fakler et al., 1995), which can be accounted for by a simple model where blocker and (several) K^+ ions displace one another in the long inner pore (defined here as extending from the intracellular end of the pore to the intracellular end of the K^+ selectivity filter). The strong voltage dependence results primarily from multiple K^+ ions traversing the transmembrane electric field (for review see Lu, 2004) that drops mainly across the ion selectivity filter. Such a blocker-K^+ mutual displacement model quantitatively accounts for the defining feature of inward rectification, namely that, for a given intracellular K^+ concentration ($[K^+]_{int}$), channel conductance is an exponential function of the difference between membrane voltage and the K^+ equilibrium potential ($V_m - E_K$) (Guo et al., 2003).

The first clue to a possible mechanism came from the study of Armstrong and Binstock (1965) who showed that intracellular TEA blocks voltage-activated K^+ channels of squid giant axon in a voltage-dependent manner, rendering them inwardly rectifying. Two decades later, intracellular Mg^{2+} was shown to block Kir channels in a voltage-dependent manner, causing inward rectification (Matsuda et al., 1987; Vandenberg, 1987). However, the voltage dependence of Mg^{2+} block is too weak to explain by itself the strong inward rectification observed in many cell types, and, furthermore, significant rectification persists in the nominal absence of Mg^{2+}. Thus, the concept of intrinsic channel gating was invoked (for review see Lu, 2004). Little progress was made in the search for additional blockers until intracellular polyamines were found to block the channels in a strongly voltage-dependent manner (Ficker et al.,

Correspondence to Zhe Lu: zhelu@mail.med.upenn.edu

Abbreviation used in this paper: Kir, inward-rectifier K^+.

J. Gen. Physiol. © The Rockefeller University Press • 0022-1295/2005/04/413/14 $8.00
Volume 125 April 2005 413–426
http://www.jgp.org/cgi/doi/10.1085/jgp.200409242

1994; Lopatin et al., 1994; Fakler et al., 1995). More recently, residual apparent intrinsic rectification in heterologously expressed wild-type IRK1 channels in the nominal absence of Mg^{2+} and polyamines has been traced to the presence of contaminating cationic blockers in the commonly employed recording solutions (Guo and Lu, 2000b, 2002). Therefore, inward rectification in IRK1 channels reflects nothing but strongly voltage-dependent channel block.

For high-affinity binding of cationic blockers, an acidic residue at a seemingly conserved site within the second transmembrane (M2) segment of Kir channels is important (Lopatin et al., 1994; Lu and MacKinnon, 1994; Stanfield et al., 1994; Wible et al., 1994). In the case of ROMK1 (Kir1.1), an acidic residue at position 171 in M2 confers a much higher affinity for blocking ions than a neutral residue, while a basic residue renders the channel essentially insensitive. On the basis of these findings, it was proposed that residue 171 affects the binding of blocking ions through an electrostatic mechanism (Lu and MacKinnon, 1994), a conclusion further supported by the fact that substituting an acidic residue at any of a number of sites in M2 enhances rectification (Guo et al., 2003; Kurata et al., 2004).

Additionally, mutations at certain acidic residues (E224 and E299) in the COOH terminus of IRK1 affect the binding of intracellular blocking ions (Taglialatela et al., 1994, 1995; Yang et al., 1995; Kubo and Murata, 2001; for structural studies see Nishida and MacKinnon, 2002; Kuo et al., 2003). Replacing both residues with neutral ones reduces channel affinity for all linear diamines (bis-alkylamines), long or short, uniformly by ~1 kcal/mole (Guo and Lu, 2003; Guo et al., 2003). The consistency of the (modest) drop in interaction energy implies that E224 and E299 interact electrostatically in a uniform manner with one of the amine groups, i.e., that one group is always positioned at a comparable (unknown) distance from the residues. It does not imply that E224 and E299 cause the amine group to reside at that location; other (perhaps stronger) forces must also be at play, and the measurable interaction between the charged residues and the amine group is a mere consequence of their relative position and serves as an experimental indicator in the quoted studies. Much less does it imply that the amine group is "fixed" by the residues in their immediate vicinity. Of the two amine groups of linear diamines, the interaction with E224 and E299 must involve the trailing amine. Indeed, the coupling coefficient Ω (Hidalgo and MacKinnon, 1995) between linear diamines and residue D172 (which is located more externally in the so-called cavity but still internal to the ion selectivity filter) rises sharply as alkyl chain length exceeds C6, peaks at C9 ($RT\ln \Omega \approx 1.5$ kcal/mole), and drops again for longer chains (Guo et al., 2003; a different pattern has been reported for Kir6.2, as will be discussed later). Thus, among all diamines, the leading amine of C9 appears to approach D172 most closely, whereas the dropoff likely reflects the leading amine group overshooting D172 (and/or alkyl chain buckling). With their trailing amine invariably positioned near the same locus on the cytoplasmic side of the IRK1 pore and their leading amine extending further into the cavity toward the selectivity filter, diamines of increasing length displace an increasing number of K^+ ions out of the long inner pore and across the selectivity filter, thereby endowing the block with increasing voltage dependence (apparent valence). This does not imply that K^+ ions move in single file through the inner pore, only that they be displaced by the protruding blocker. If the leading end of longer amines such as C12 (whose length equals spermine's) penetrated deep into the selectivity filter, the voltage dependence of channel block would continue to rise beyond C9. Instead, the apparent valence of channel block reaches ~5 at C9 but rises no further for longer alkyl chains (the apparent valence of block by spermine is also ~5) (Guo and Lu, 2003; Guo et al., 2003). These observations imply that amine blockers seldom reach deep into the selectivity filter (Guo and Lu, 2000a).

The notion that residues E224 and E299 interact with the trailing amine of alkyl di- and monoamines has been termed counterintuitive because "it is not intuitively apparent why the monoamine would enter the water-filled cavity alkyl tail first" (Kurata et al., 2004; cf. John et al., 2004). The following observations are, however, more readily explained by the tail-first monoamine-binding orientation (Guo et al., 2003). First, the "on" rate constants for block by alkyl monoamines (at 0 mV) are ~600-fold lower than those of the corresponding diamines, rather than twofold as expected on statistical grounds if an amine group were always leading. The much lower "on" rate constants for monoamines fit the expectation that without electrostatic focusing, the alkyl chain has a low probability of finding the pore and forming the encounter complex. Second, while the apparent valence of block increases with monoamine chain length, the interaction energy with D172 remains constant. Third, the difference in maximal valence of block (4 versus 5) between linear mono- and diamines is economically explained by the failure of a naked alkyl chain, unlike one bearing a charged amine group, to displace a K^+ ion present in the water-filled cavity. Lastly, the proposed model is energetically plausible because most of the binding energy (especially for long alkylamines) derives from hydrophobic interactions (Guo et al., 2003). In fact, neutralizing D172 reduces the (electrostatic) interaction energy for the diamine C9 by ~2 kcal/mole, while in the presence of D172, the difference in interaction energy between mono- and diamines of identical alkyl chain length is also ~2 kcal/mole.

Importantly, independent of a detailed interpretation of the relative position of various amine blockers in the IRK1 pore, the fact that the observed valence of IRK1 block by amines, be they divalent or monovalent, rises (in apparent increments of ~1) with blocker length to as high as 4–5 (Guo and Lu, 2003; Guo et al., 2003) suggests strongly that the voltage dependence derives primarily from K^+ ion charges, and not blocker charges themselves, moving across the selectivity filter when an amine blocker binds or unbinds. As a further test of this proposal, we asked whether channel block by decane-*bis*-trimethylammonium (bis-QA_{C10}; Miller, 1982), with a length equal to that of C12 or spermine but a head group (~6 Å) much wider than what the ion selectivity filter (~3 Å) can accommodate, also exhibits a valence ~5.

The voltage dependence of the inhibition rate constant for all amine blockers examined is remarkably low (<1; Guo and Lu, 2003; Guo et al., 2003). This would suggest that the ion conduction pore in IRK1 becomes blocked as soon as an amine blocker encounters the innermost K^+ ion and before, in (a) more steeply voltage-dependent step(s), it reaches a deeper and more stable position in the long inner pore. If there are indeed two (or more) serially-related blocked states (Guo et al., 2003; Guo and Lu, 2003) several consequences can be anticipated: (1) the voltage dependence of steady-state IRK1 block should itself increase with voltage as positive voltage favors formation of deeper blocked states where more K^+ ions are displaced, (2) individual rate constants and valences may, under favorable experimental conditions, be extracted, and (3) except by coincidence, the ratio of apparent unblock and block rate constants will not match the (overall) equilibrium dissociation constant. These features of the model will also be examined. Where appropriate, we will also discuss other proposed models in which it is assumed that polyamines mainly bind deep in the selectivity filter, or that the binding of polyamines produces a "partial conductance" state (Xie et al., 2002, 2003; Dibb et al., 2003; Kurata et al., 2004; cf. John et al., 2004).

MATERIALS AND METHODS

Molecular Biology and Oocyte Preparation

The cDNA of IRK1 (Kubo et al., 1993) was subcloned in pGEM-HESS plasmid (Liman et al., 1992). The cRNA was synthesized with T7 polymerase (Promega) using linearized cDNA as a template. Oocytes harvested from *Xenopus laevis* (*Xenopus* One) were incubated in a solution containing NaCl, 82.5 mM; KCl, 2.5 mM; $MgCl_2$, 1.0 mM; HEPES (pH 7.6), 5.0 mM; and collagenase, 2–4 mg/ml. The oocyte preparation was agitated at 80 rpm for 60–90 min. It was then rinsed thoroughly and stored in a solution containing NaCl, 96 mM; KCl, 2.5 mM; $CaCl_2$, 1.8 mM; $MgCl_2$, 1.0 mM; HEPES (pH 7.6), 5 mM; and gentamicin, 50 μg/ml. Defolliculated oocytes were selected and injected with RNA at least 2 and 16 h, respectively, after collagenase treatment. All oocytes were stored at 18°C.

Recordings and Solutions

Macroscopic currents were recorded at ambient temperature from inside-out membrane patches of *Xenopus* oocytes heterologously expressing IRK1 channels using an Axopatch 200B amplifier (Axon Instruments, Inc.), filtered at 5–10 kHz, and sampled at 40–100 kHz using an analogue-to-digital converter (Digidata 1322A; Axon Instruments, Inc.) interfaced with a personal computer. pClamp8 software was used to control the amplifier and acquire the data. During current recording, the voltage across the membrane patch was first hyperpolarized from the 0-mV holding potential to −100 mV, and then stepped to various test voltages between −100 and 100 mV and back to 0 mV. To examine unblock kinetics, membrane voltage was first depolarized from the 0 mV holding potential to 100 mV and then stepped to various test voltages and back to 0 mV. Background leak current correction was performed as previously described (Lu and MacKinnon, 1994; Guo and Lu, 2000b). The recording solution contained (in mM): 5 K_2EDTA, 10 "K_2HPO_4 + KH_2PO_4" in a ratio yielding pH 8.0, and sufficient KCl to bring total K^+ concentration to 100 mM (Guo and Lu, 2000b, 2002). Na_2EDTA and 10 "Na_2HPO_4 + NaH_2PO_4" were used to make the low K^+ solution, and the final concentrations of K^+ and Na^+ were 10 and 90 mM, respectively. To reduce channel rundown, the intracellular solution contained 5 mM fluoride and 0.1 mM vanadate (Huang et al., 1998). All chemicals were purchased from Fluka Chemical Corp.

RESULTS

For both bis-QA_{C10} and spermine, we will first present analyses of steady-state block from which we determine the apparent equilibrium dissociation constants at 0 mV and the associated voltage dependence, followed by analyses of current transients to determine block/unblock rate constants and their voltage dependence. For both blockers, it appears that the voltage dependence of their affinity is nonuniform over the voltage range examined, a strong indication that blocker-channel interaction involves more than a single voltage-dependent step. This conclusion is reinforced by the fact that the (overall) equilibrium dissociation constant differs from the ratio of apparent unblock and block rate constants. Further analyses of all experimental parameters and their interpretations will be presented later in DISCUSSION.

Channel Block by Decane-bis-trimethylammonium

Fig. 1 shows IRK1 currents recorded in the absence or presence of two concentrations of intracellular bis-QA_{C10}. At 10 μM bis-QA_{C10}, only outward currents are inhibited but, at 10 mM, inward currents are also somewhat inhibited. Like di- and polyamines, bis-QA_{C10} inhibits the IRK1 channels in a strongly voltage-dependent manner and, consequently, renders the I–V curve inwardly rectifying (Fig. 2 A). As shown for four representative voltages, we determined the apparent equilibrium dissociation constant ($^{app}K_d$) at a

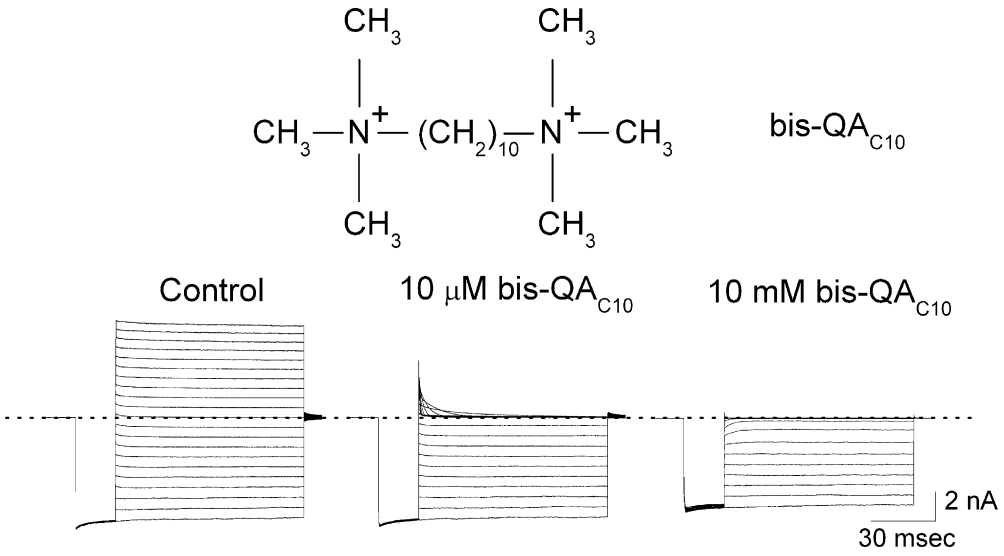

FIGURE 1. Inhibition of IRK1 currents by bis-QA_{C10}. Chemical structure of bis-QA_{C10} is shown on top. Current traces were recorded from a single patch in the absence (control) or presence of bis-QA_{C10} at the concentrations indicated. Currents were elicited by stepping membrane voltage from the 0-mV holding potential to −100 mV and then to test voltages between −100 and +100 mV in 10-mV increments before returning it to the holding potential. Dotted line indicates zero current.

given voltage by fitting the plot of normalized current against bis-QA_{C10} concentration with a hyperbolic equation (Fig. 2 B). To illustrate the voltage dependence of ${}^{app}K_d$, we plotted its natural logarithm against membrane voltage (Fig. 2 C). The plot is nonlinear: its slope, which reflects the voltage dependence of ${}^{app}K_d$, is itself voltage dependent, as expected for a model where two (or more) serially related blocked states are connected by voltage-dependent steps. The value of (overall) ${}^{app}K_d$ (0 mV) is 9.4×10^{-5} M (see DISCUSSION for details).

Block and unblock kinetics were studied by applying large voltage steps. Fig. 3 A shows the effect on K^+ current of stepping the voltage from −100 to 70 mV in the absence or presence of 0.1 μM bis-QA_{C10}. The transient in the presence of blocker is fitted with a single-exponential function (the first 3 ms of the current trace was omitted because voltage clamp or capacitance correction may have been inadequate). The fit intersects the current not blocked at the time when membrane depolarization began, and the transient thus exhibits no detectable instantaneous decline or delay in response to the voltage step. To analyze the concentration dependence of the rate of inhibition, we plotted the reciprocal of the time constants for channel block ($1/\tau_{on}$), obtained from fits such as in Fig. 3 A, against bis-QA_{C10} concentration for four representative voltages (Fig. 3 B). From the slope of the linear fit for each voltage, we obtained the apparent second-order rate constant (${}^{app}k_{on}$) for channel block. To determine the latter's voltage dependence, we plotted its natural logarithm against membrane voltage (Fig. 3 C) and fitted the relation with a Boltzmann function, obtaining $k_{on}(0\ mV) = 1.63 \times 10^7\ M^{-1}s^{-1}$ and apparent valence (z_{on}) = 0.73.

We next studied the kinetics of recovery from channel block. Fig. 4 A shows the current transient elicited in the presence of 1 mM bis-QA_{C10} by stepping membrane voltage from 100 mV (where the channels are fully blocked) to −40 mV with data during the first 0.3 ms omitted. The single-exponential fit superimposed on the data intersects zero current at the time when membrane hyperpolarization began, which signifies that there is no detectable instantaneous current decline or delay in response to the voltage step. Similar experiments were performed at three bis-QA_{C10} concentrations and five voltages, and we plotted the natural logarithm of $1/\tau_{off}$, obtained from fits such as shown in Fig. 4 A, against bis-QA_{C10} concentration for each voltage (Fig. 4 B). Since $1/\tau_{off}$ is independent of bis-QA_{10} concentration as expected, we used the mean of the values obtained at three concentrations to estimate ${}^{app}k_{off}$ for a given voltage. To obtain the voltage dependence of ${}^{app}k_{off}$, we plotted its natural logarithm against membrane voltage in Fig. 4 C. The line through the data is a fit of the Boltzmann function, yielding $k_{off}(0\ mV) = 1.06 \times 10^2\ s^{-1}$ and $z_{off} = 1.46$. It is informative to compare the ratio of experimentally determined k_{off} and k_{on} at 0 mV (6.5×10^{-6} M) with the experimentally determined overall ${}^{app}K_d(0\ mV) = 9.4 \times 10^{-5}$ M. The ~15-fold difference between the two values strongly suggests (see DISCUSSION) that the blocking reaction involves more than a single step.

The question has arisen (see DISCUSSION) of whether Kir channel blockers invade the ion selectivity filter. In the case of bis-QA_{C10} with ~6-Å-wide head groups, this would necessarily entail some structural rearrangement of the ~3-Å-wide filter. To test whether the binding of bis-QA_{C10} distorts the ion selectivity filter enough to affect its predilection for K^+, we examined hyperpolarization-induced current transients in the presence of intracellular bis-QA_{C10} and of either 100 mM extracellular K^+ or 10 mM K^+ plus 90 mM Na^+

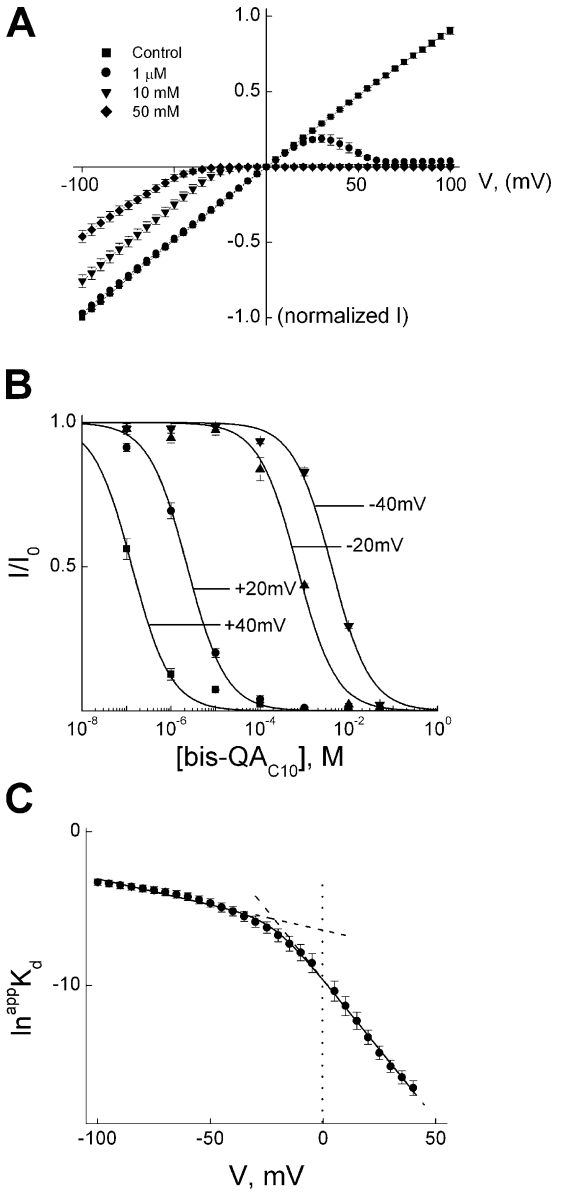

FIGURE 2. Voltage dependence of steady-state IRK1 block by bis-QA_{C10}. (A) Averaged I–V curves (mean ± SEM; $n = 6$) determined at the end of test pulses in the absence (control) or presence of various concentrations of bis-QA_{C10}. (B) The fraction of current not blocked is plotted against bis-QA_{C10} concentration at the four representative voltages indicated. Curves through the data represent the equation $I/I_o = {}^{app}K_d/({}^{app}K_d + [\text{bis-QA}_{C10}])$. (C) The natural logarithm of ${}^{app}K_d$ is plotted against membrane voltage. The line through the data is a fit of Eq. 1a, yielding $K_1 = 3.10 \pm 0.11 \times 10^{-3}$ M (mean ± SEM; $n = 6$), $K_2 = 3.04 \pm 0.72 \times 10^{-2}$, $Z_1 = 0.82 \pm 0.03$, and $Z_2 = 3.63 \pm 0.20$, where the overall ${}^{app}K_d$ (0 mV) $= K_1K_2$. The dashed lines indicate the limiting slopes, and the vertical dotted line indicates zero voltage.

(Fig. 5). The curves superimposed on the transients are single-exponential fits. The unblock kinetics are over an order magnitude faster in 100 mM K^+, which suggests that IRK1 complexed with bis-QA_{C10} retains its K^+ selectivity.

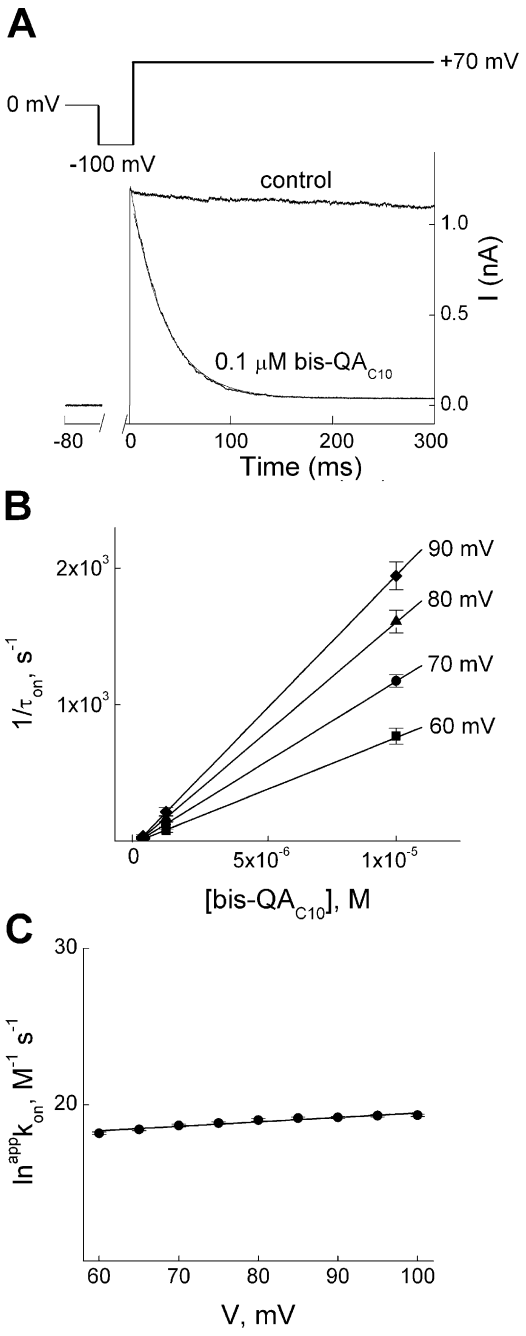

FIGURE 3. Kinetics of depolarization-induced IRK1 block by bis-QA_{C10}. (A) Current transient elicited by stepping membrane voltage from −100 to 70 mV in the absence (control) or presence of 0.1 μM bis-QA_{C10}; the first 3 ms of the transient in the presence of bis-QA_{C10} was omitted (see RESULTS). The curve superimposed on the transient (and back extrapolated to the start of depolarization) is a single-exponential fit. (B) The reciprocal of the time constant (mean ± SEM, $n = 6$) for channel block ($1/\tau_{on}$), obtained as shown in A, is plotted against bis-QA_{C10} concentration (0.1, 1, and 10 μM) for four voltages. The lines through the data are linear fits whose slope gives the apparent second-order rate constant (${}^{app}k_{on}$) for blocker binding. (C) The natural logarithm of ${}^{app}k_{on}$ from B is plotted against membrane voltage. The line through the data is a fit of the Boltzmann function, yielding $k_{on}(0\text{ mV}) = 1.63 \pm 0.37 \times 10^7\ M^{-1}s^{-1}$ (mean ± SEM, $n = 6$) and $z_{on} = 0.73 \pm 0.07$.

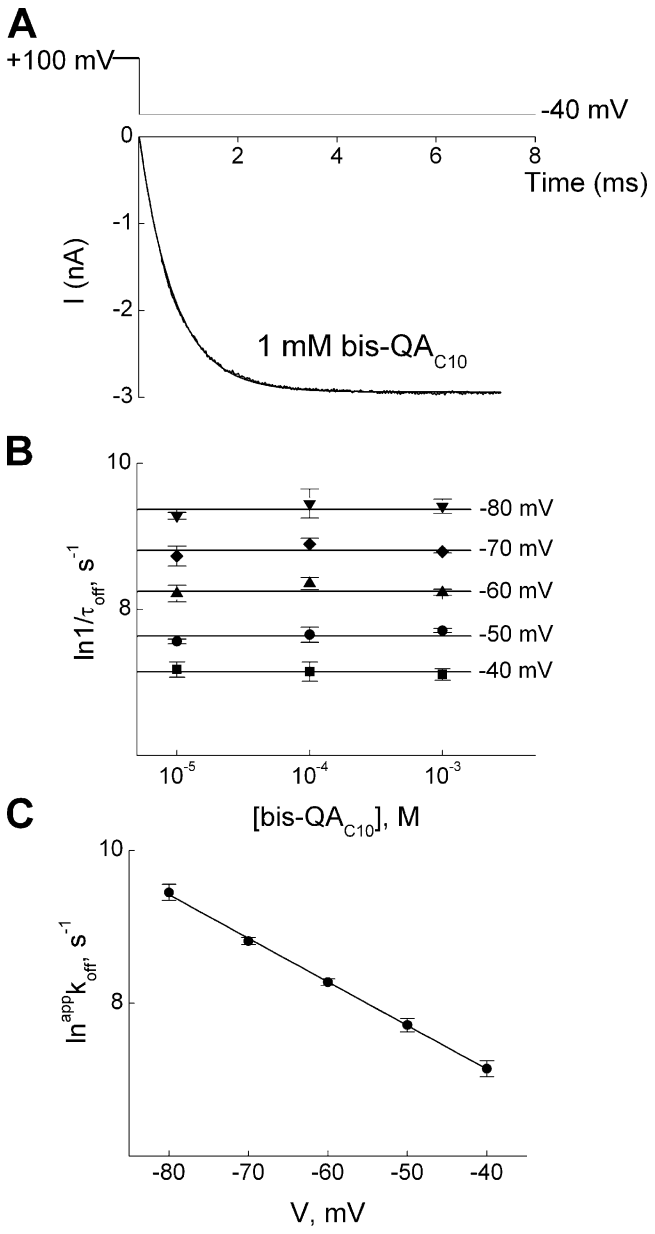

FIGURE 4. Kinetics of hyperpolarization-induced unblock of IRK1 channels in the presence of bis-QA_{C10}. (A) Current transient elicited by stepping membrane voltage from 100 to −40 mV in the presence of 1 mM bis-QA_{C10}, where the first 0.3 ms of the trace was omitted. The curve superimposed on the transient (and back extrapolated to the start of depolarization) is a single-exponential fit. (B) The natural logarithm of the reciprocal of the time constants (mean ± SEM; $n = 3$) for channel unblock ($1/\tau_{off}$, an estimate of the apparent off rate constant $^{app}k_{off}$), obtained as shown in A, is plotted against bis-QA_{C10} concentration for five voltages. The lines through the data represent, for a given voltage, the average over the three concentrations tested. (C) The natural logarithm of the average $^{app}k_{off}$ from B is plotted against membrane voltage. The line through the data is a fit of the Boltzmann function, yielding $k_{off}(0\ mV) = 1.06 \pm 0.07 \times 10^2\ s^{-1}$ (mean ± SEM, $n = 3$) and $z_{off} = 1.46 \pm 0.02$.

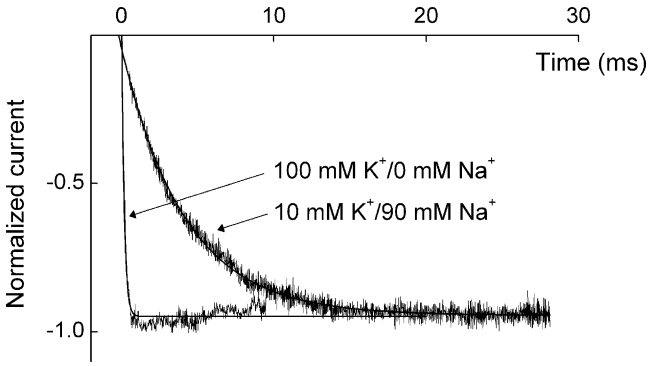

FIGURE 5. Extracellular K^+ sensitivity of hyperpolarization-induced unblock kinetics in the presence of bis-QA_{C10}. Normalized current transients elicited by stepping membrane voltage from 100 to −70 mV in the presence of 0.1 mM bis-QA_{C10} and either 100 or 10 mM extracellular K^+, where the first 0.1 or 0.3 ms of the record was omitted. The 10 mM K^+ extracellular solution contained 90 mM Na^+; the intracellular solution contained 100 mM K^+ in both cases. The curves superimposed on the current transients are single-exponential fits. From these and similar fits, we obtained time constants of 0.15 ± 0.02 and 4.59 ± 0.27 ms (mean ± SEM; $n = 3$ and 4) for 100 and 10 mM extracellular K^+, respectively.

Channel Block by Spermine

We similarly examined, for comparison, the steady-state and presteady-state kinetics of channel block by intracellular spermine. Fig. 6 A shows IRK1 currents recorded in the absence or presence of 100 μM spermine. As shown previously (Lopatin et al., 1995; Xie et al., 2002), at this high concentration spermine inhibits both inward and outward currents. The relation (Fig. 6 B) between the fraction of current not blocked and membrane voltage exhibits both a shallow and a steep phase and, consequently, requires an equation with two Boltzmann terms, again suggesting that channel-blocker interaction involves more than a single voltage-dependent step. The value of overall $^{app}K_d(0\ mV)$ is 1.9×10^{-6} M (see DISCUSSION for details).

Fig. 7 A shows the effect on membrane current of stepping the voltage from −100 to 80 mV in the absence or presence of 0.1 μM spermine. The transient in the presence of blocker is fitted with a single-exponential function (the first 3 ms of the current trace was omitted). The fit intersects the current not blocked at the time when membrane depolarization began, and the transient thus exhibits no detectable instantaneous decline or delay in response to the voltage step. As shown for bis-QA_{C10} (Fig. 3 B) and for spermine (Guo and Lu, 2003), we obtained $^{app}k_{on}$ from the slope of a linear plot of $1/\tau_{on}$ against spermine concentration. The natural logarithm of $^{app}k_{on}$ is plotted against membrane voltage in Fig. 7 B. A fit of the Boltzmann function yields $k_{on}(0\ mV) = 6.47 \times 10^8\ M^{-1}s^{-1}$ and $z_{on} = 0.16$.

To illustrate spermine unblocking kinetics, we show current transients elicited in the presence of 1 μM

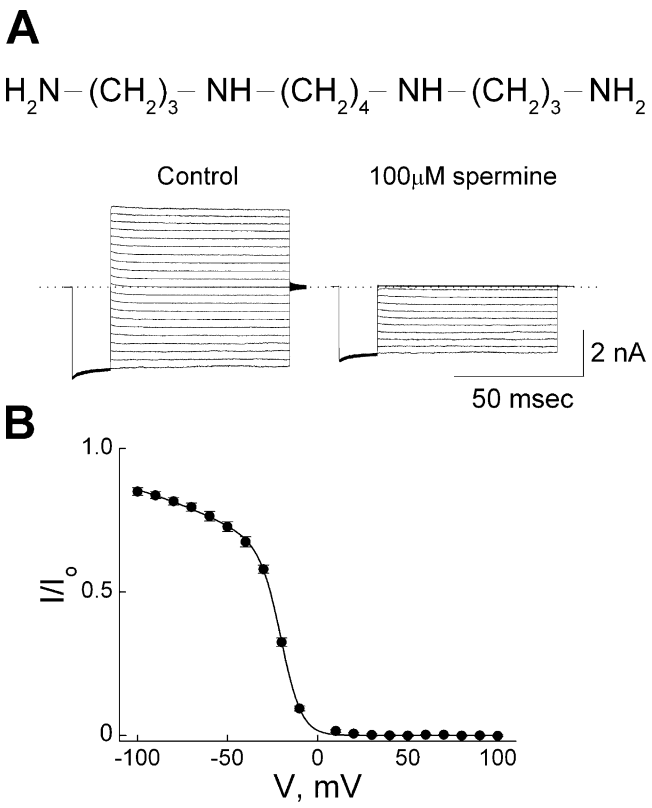

FIGURE 6. Voltage dependence of steady-state IRK1 block by spermine. (A) Chemical structure of spermine is shown on top. IRK1 currents recorded from a single patch in the absence (control) then presence of 100 μM spermine were elicited with the same voltage protocol as in Fig. 1. Dotted line indicates zero current. (B) The fraction of current (mean ± SEM, $n = 9$) not blocked by 100 μM spermine is plotted against membrane voltage. The curve through the data is a fit of Eq. 1, yielding $K_1 = 1.30 \pm 0.06 \times 10^{-4}$ M (mean ± SEM, $n = 9$), $K_2 = 1.44 \pm 0.13 \times 10^{-2}$, $Z_1 = 0.40 \pm 0.02$, and $Z_2 = 4.23 \pm 0.13$, where the overall $^{app}K_d$ (0 mV) = K_1K_2.

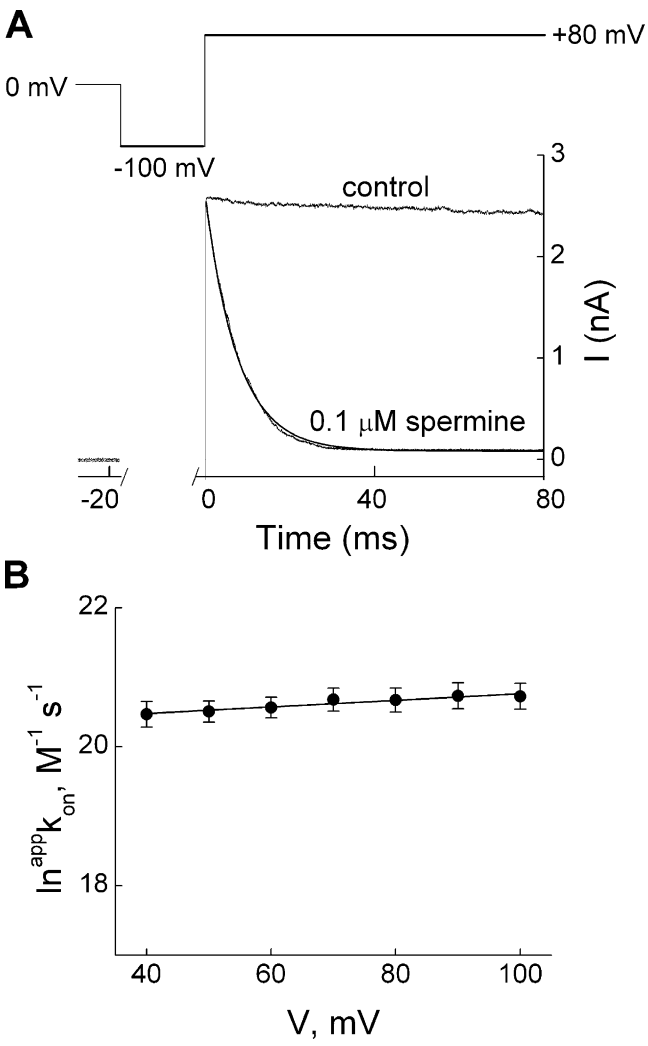

FIGURE 7. Kinetics of depolarization-induced IRK1 block by spermine. (A) Current transient elicited by stepping membrane voltage from −100 to 80 mV in the absence (control) or presence of 0.1 μM spermine, where the first 3 ms of the record in the presence of spermine was omitted, and the curve superimposed on the transient is a single-exponential fit. (B) The natural logarithm of $^{app}k_{on}$, obtained with the method shown in Fig. 3, B and C, from data such as shown in A, is plotted against membrane voltage. The line through the data is a fit of the Boltzmann function, yielding $k_{on}(0\text{ mV}) = 6.47 \pm 0.30 \times 10^8\ M^{-1}s^{-1}$ (mean ± SEM, $n = 23$) and $z_{on} = 0.16 \pm 0.02$.

spermine by stepping membrane voltage from 100 mV (where current is completely inhibited) to −40 mV (Fig. 8 A). The curve superimposed on the data is a single-exponential fit which, as was the case for bis-QA_{C10}, extrapolates to zero current at the start of hyperpolarization. Thus, there is no detectable instantaneous current decline or delay in response to the voltage step. We performed similar experiments at three spermine concentrations and six voltages, and plotted the natural logarithm of $1/\tau_{off}$, obtained from the fits against spermine concentration for each voltage (Fig. 8 B). Since $1/\tau_{off}$ is independent of spermine concentration as expected, we used the mean of the values obtained at the three concentrations to estimate $^{app}k_{off}$ for a given voltage, and plotted its natural logarithm against membrane voltage in Fig. 8 C. The line through the data is a fit of the Boltzmann function, yielding $k_{off}(0\text{ mV}) = 5.34 \times 10^2\ s^{-1}$ and $z_{off} = 1.18$. In the case of spermine, the experimentally determined overall $^{app}K_d$ (Fig. 6 B) and k_{off}/k_{on} (Fig. 8 C; Fig. 7 B), all at 0 mV, differ by a factor of ~2.

DISCUSSION

The voltage dependence of IRK1 block by intracellular cations such as spermine has been suggested to arise primarily from displaced K^+ ions, not the blockers themselves, traversing the transmembrane electrical field, which mainly drops across the selectivity filter. Also, since the ion conduction pore in IRK1 becomes blocked as soon as an amine blocker encounters the in-

nermost K^+ ion and before it reaches a deeper, energetically more stable position, there must exist at least two serially related blocked states that can potentially be identified experimentally. These two features of the blocker-K^+ displacement model predict (1) that, provided its leading end can reach the cavity, bis-QA_{C10} with head groups much wider than the selectivity filter will block IRK1 channels with a valence comparable to that of spermine (a molecule of similar length), and (2) that this apparent valence itself will be voltage dependent. Both predicted phenomena are indeed observed experimentally.

We first examine IRK1 block by bis-QA_{C10}. Fig. 2 C shows that the voltage dependence of channel block by bis-QA_{C10} increases with membrane depolarization, consistent with the existence of at least two blocked states connected by voltage-dependent steps. In a minimal model (Fig. 9) containing one open (Ch) and two consecutive blocked states (ChB_1 and ChB_2), the shallow limiting slope of a plot of ${}^{app}K_d$ against V_m at negative voltages reflects valence Z_1 associated with the first blocking transition, whereas the steep limiting slope at positive voltages reflects the sum of Z_1 and Z_2, the latter associated with the transition between blocked states. Extrapolation of the shallow limiting slope to 0 mV yields the equilibrium dissociation constant (K_1) for the first blocking transition, whereas that of the steep phase gives the product of K_1 and K_2 (the notation "0 mV" will henceforth be omitted for simplicity). To evaluate the energetics of each transition, both limiting phases must be explored. If the objective is only to study the overall energetics of the blocking process, the limiting phase at positive voltages suffices; the analysis then only requires an equation containing a single Boltzmann term, where the (overall) ${}^{app}K_d(0\ mV) = K_1K_2$ and ${}^{app}Z = Z_1 + Z_2$. Interpretation of data intermediate between the two limiting phases is not straightforward because they reflect a mixture of properties of the two blocked states, as described by Eq. 1.

For the model of Fig. 9, the steady-state fraction of current not blocked is given by

$$\frac{I}{I_{MAX}} = \frac{1}{1 + \frac{[B]}{{}^{app}K}}, \qquad (1)$$

where

$${}^{app}K = \left(\frac{1}{K_1 e^{-\frac{Z_1 F V_m}{RT}}} + \frac{1}{K_1 K_2 e^{-\frac{(Z_1 + Z_2) F V_m}{RT}}} \right)^{-1}. \qquad (1a)$$

A fit of Eq. 1a to the plot in Fig. 2 C yields the equilibrium constants for the two transitions $K_1 = 3.10 \times 10^{-3}$ M and $K_2 = 3.04 \times 10^{-2}$, with valences $Z_1 = 0.83$ and $Z_2 = 3.63$.

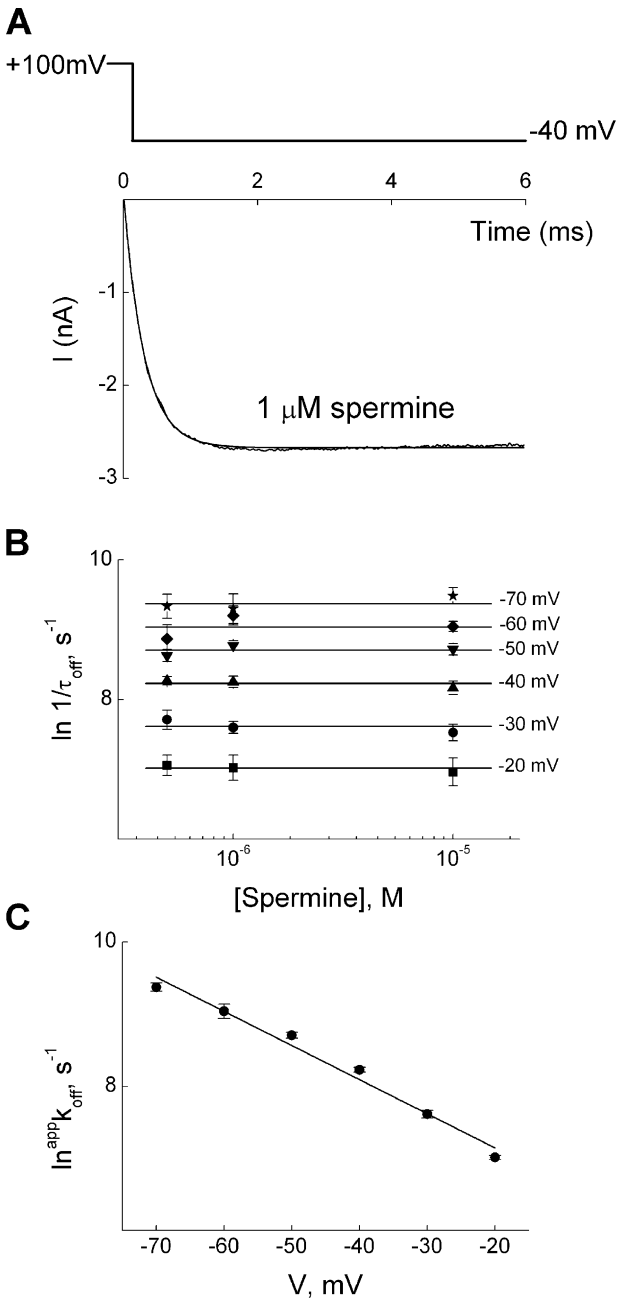

FIGURE 8. Kinetics of hyperpolarization-induced unblock of IRK1 channels in the presence of spermine. (A) Current transient elicited by stepping membrane voltage from 100 to −40 mV in the presence of 1 μM spermine, where the first 0.3 ms of the trace was omitted. The curve superimposed on the transient is a single-exponential fit. (B) The natural logarithm of the reciprocal of the time constants (mean ± SEM; $n = 6$) for channel unblock ($1/\tau_{off}$, an estimate of the apparent rate constant ${}^{app}k_{off}$), obtained as shown in A, is plotted against spermine concentration for six voltages. The lines through the data represent, for a given voltage, the average over the three concentrations tested. (C) The natural logarithm of average ${}^{app}k_{off}$ from B is plotted against membrane voltage. The line through the data is a fit of the Boltzmann function, yielding $k_{off}(0\ mV) = 5.34 \pm 0.80 \times 10^2\ s^{-1}$ (mean ± SEM, $n = 6$) and $z_{off} = 1.18 \pm 0.08$.

The apparent second-order rate constant $^{app}k_{on}$ for formation of the first blocked state (obtained from Fig. 3 C) is $k_1 = 1.63 \times 10^7\ M^{-1}s^{-1}$ with valence $^{app}z_{on} = z_1 = 0.73$, from which we calculate the off rate constant $k_{-1} = k_1K_1 = 5.05 \times 10^4\ s^{-1}$ with valence $z_{-1} = Z_1 - z_1 = 0.10$. The apparent unblocking rate constant $^{app}k_{off} = 1.06 \times 10^2\ s^{-1}$ (obtained from Fig. 4 C) is >400 times slower than k_{-1} just computed and, therefore, a valid approximation of k_{-2}, with associated valence $^{app}z_{off}$ (1.46) = z_{-2}. From these, we compute the rate constant for formation of the second blocked state $k_2 = k_{-2}/K_2 = 3.49 \times 10^3\ s^{-1}$ with valence $z_2 = Z_2 - z_{-2} = 2.17$. These kinetic parameters for bis-QA_{C10} block/unblock are tabulated in Fig. 9. We note that both the bis-QA_{C10} block (Fig. 3 A) and unblock (Fig. 4 A) transients exhibit single-exponential time courses without sudden jumps or delays. Thus, a model in which one blocker blocks one channel suffices. We also note that the ratio of the experimental "off" and "on" rate constants at 0 mV (from Fig. 4 C and Fig. 3 C, respectively), $^{app}k_{off}/^{app}k_{on} = (1.06 \times 10^2\ s^{-1})/(1.63 \times 10^7\ M^{-1}s^{-1}) = 6.50 \times 10^{-6}$ M, differs 14.5-fold from the experimental value of the overall $^{app}K_d$(0 mV), $K_1K_2 = (3.10 \times 10^{-3}\ M) \times (3.04 \times 10^{-2}) = 9.42 \times 10^{-5}$ M (Fig. 2 C). Such wide divergence conclusively eliminates single-step models of channel block by bis-QA_{C10}.

For comparison, we now analyze spermine block. Lopatin et al. (1995) reported that in the presence of spermine, a plot of HIRK1 (Kir2.3) current not blocked against membrane voltage exhibits a shallow and a steep phase (initially interpreted as reflecting sequential binding of two spermine molecules in the pore). A similar observation was made in IRK1 (Xie et al., 2002). Such variation, with membrane voltage, of the voltage dependence of channel block is expected for a model in which an increasing number of K^+ ions are displaced across the selectivity filter by a long amine as it penetrates deeper into the pore. Fitting the plot (Fig. 6 B) of fraction of IRK1 current not blocked by 100 μM spermine against membrane voltage with Eq. 1, we obtain $K_1 = 1.30 \times 10^{-4}$ M and $K_2 = 1.44 \times 10^{-2}$, with valences $Z_1 = 0.40$ and $Z_2 = 4.23$. Since the greater part of the voltage dependence of channel block by spermine (and by bis-QA_{C10}) is associated with K_2, it follows that mutual displacement of blocker and K^+ ions must take place mainly during the transition between blocked states as the blocker travels along the long inner pore.

A reasoning similar to that above for bis-QA_{C10} yields, from Fig. 7 B, rate constant $^{app}k_{on}$ for spermine $k_1 = 6.47 \times 10^8\ M^{-1}s^{-1}$ with valence $^{app}z_{on} = z_1 = 0.16$. These values allow computation of $k_{-1} = k_1K_1 = 8.41 \times 10^4\ s^{-1}$ with valence $z_{-1} = Z_1 - z_1 = 0.24$. Since again the apparent unblocking rate constant $^{app}k_{off}$ obtained from Fig. 8 C ($5.34 \times 10^2\ s^{-1}$) is over 100-fold slower

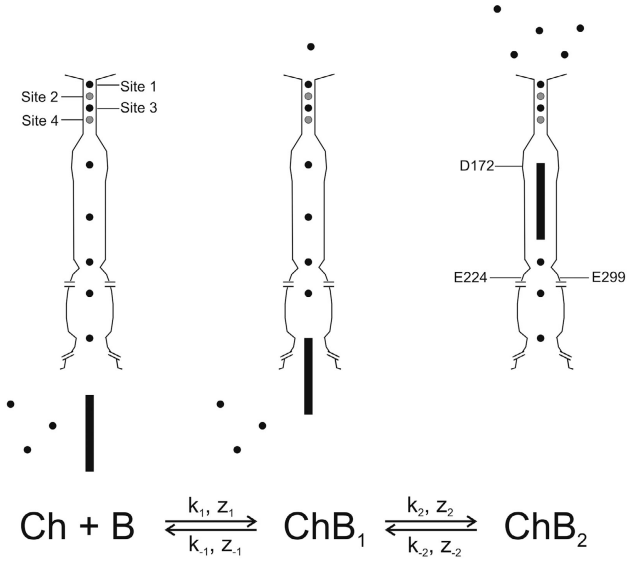

	bis-QA_{C10}	spermine
k_1	$1.63 \times 10^7\ M^{-1}\ s^{-1}$	$6.47 \times 10^8\ M^{-1}\ s^{-1}$
k_2	$3.49 \times 10^3\ s^{-1}$	$3.71 \times 10^4\ s^{-1}$
k_{-1}	$5.05 \times 10^4\ s^{-1}$	$8.41 \times 10^4\ s^{-1}$
k_{-2}	$1.06 \times 10^2\ s^{-1}$	$5.34 \times 10^2\ s^{-1}$
z_1	0.73	0.16
z_2	2.17	3.05
z_{-1}	0.10	0.24
z_{-2}	1.46	1.18

FIGURE 9. Kinetic model for spermine or bis-QA_{C10} block of the IRK1 channel. Binding of a blocker (B) to a channel (Ch) produces two sequentially related blocked states (ChB_1 and ChB_2). Top, cartoon representing the three channel states (see also Guo et al., 2003; Guo and Lu, 2003; Lu, 2004). The position of K^+ ions (maximally totaling five) in the inner pore is arbitrary. The rate constants (k_x) and associated valences (z_x) for each blocker are tabulated below.

than k_{-1} just computed, it is a valid approximation of k_{-2}, with associated valence $^{app}z_{off} = z_{-2} = 1.18$. From these we then obtain $k_2 = k_{-2}/K_2 = 3.71 \times 10^4\ s^{-1}$ and $z_2 = Z_2 - z_{-2} = 3.05$. These kinetic parameters for spermine block/unblock are also tabulated in Fig. 9. We note as well the single-exponential character of both the spermine block (Fig. 7 A) and unblock (Fig. 8 A) transients without sudden jumps or delays. Thus, a model in which one blocker blocks one channel again suffices. In the case of spermine, the ratio of the experimental "off" and "on" rate constants at 0 mV (from Fig. 8 C and Fig. 7 B, respectively) is $(5.34 \times 10^2\ s^{-1})/(6.47 \times 10^8\ M^{-1}s^{-1}) = 8.3 \times 10^{-7}$ M, compared with an experimental equilibrium dissociation constant (Fig. 6 B) of $K_1K_2 = (1.30 \times 10^{-3}\ M) \times (1.44 \times 10^{-2}) =$

1.87×10^{-6} M. The accidental numerical similarity (or modest 2.3-fold difference) of these values does not in any way force assumption of a single-step reaction scheme.

Spermine and bis-QA_{C10} molecules have practically the same length but the latter has much wider (~6 Å) head groups. Wedging of bis-QA_{C10} deep into the ~3-Å-wide selectivity filter would most likely widen the filter and thus cause it to lose its K^+ selectivity. However, ${}^{app}k_{off}$ (or k_{-2}) for bis-QA_{C10} remains highly sensitive to extracellular K^+ (Fig. 5), suggesting strongly that the selectivity filter in the deeper blocked state remains K^+ selective. Thus, the likelihood of bis-QA_{C10} penetrating deep into the K^+ selectivity filter seems very low indeed. If spermine, unlike bis-QA_{C10}, occupied a significant fraction of the selectivity filter (as proposed by Dibb et al., 2003; Kurata et al., 2004; cf. John et al., 2004) in the deeper blocked state, it would display a much stronger voltage dependence than bis-QA_{C10}. In fact, the overall valences for channel block by spermine and by bis-QA_{C10} are practically identical ($Z_1 + Z_2 = 4.6$ versus 4.5). We conclude that spermine must have a low probability of penetrating "deep" into the selectivity filter, consistent with the finding that it has a very low probability of traversing the IRK1 pore (Guo and Lu, 2000a,b; Guo et al., 2003; see also below).

Our experimentally determined rate constants and apparent valences for individual transitions (Fig. 9) predict certain single-channel behaviors. First, with spermine concentration in the 10^{-4} M range, both k_1[spermine] and k_{-1} are large. Consequently, channels will transit between the open and the first blocked states too rapidly for individual current events to be resolved with the usual bandwidth, so that block will manifest itself as an apparent reduction of single-channel conductance. In the voltage range where the first blocked state predominates, this reduction will be a continuous function of spermine concentration and of membrane voltage. A second prediction is that, in the voltage range where both blocked states are populated, single-channel events must occur that reflect the slower ChB_1–ChB_2 transition. The relative population of the two blocked states as a function of voltage is given by

$$\frac{[ChB_1]}{[ChB_1] + [ChB_2]} = \frac{1}{1 + K_2 e^{\frac{Z_2 F V_m}{RT}}} \quad (2)$$

and

$$\frac{[ChB_2]}{[ChB_1] + [ChB_2]} = \frac{1}{1 + K_2 e^{-\frac{Z_2 F V_m}{RT}}}$$

Plots of these equations (Fig. 10) show that the fraction of channels in the ChB_2 state is minimal at −50 mV but then rises steeply (because $Z_2 = 4.23$ is large) with membrane depolarization. The predicted phenomena have already been observed at the single-channel level (Xie et al., 2002). First, these authors found that, at −60 mV, increasing the spermine concentration reduces the apparent single-channel conductance, while at fixed spermine concentration and voltages negative to −50 mV, apparent single-channel conductance decreases with depolarization. Second, at voltages positive to −50 mV, the channel abruptly transited to a regime of higher open-channel noise. It should be acknowledged that Xie et al. (2002) interpreted the low- and high-noise events as manifestations of partially and fully spermine-blocked channels, and argued against the possibility that apparently reduced single-channel conductance reflects inadequate recording bandwidth. Their argument was critically based on the assumption that blocking kinetics of spermine are much slower than those of TEA, because the latter compound was used as a positive control for adequate bandwidth (see also Xie et al., 2003; John et al., 2004). However (even after taking into account the 20-fold higher TEA concentration range used in the quoted study) the assumption is not justified because experimentally determined ${}^{app}k_{on}$ for spermine is approximately three orders of magnitude faster than for TEA (~10^9 $M^{-1}s^{-1}$ versus ~10^6 $M^{-1}s^{-1}$; Guo and Lu, 2001, 2003; see also Fig. 7 B).

In some cases, the rate constant of channel block may still be determined from macroscopic current transients even though block is too fast to be resolved with single-channel recordings. In the present case, spermine affinity of the first blocked state (favored over the second by hyperpolarization; Fig. 10) is quite low (0.13 mM; Fig. 6 B) so that, besides negative potentials, high concentrations of spermine are needed to populate the first blocked state. Under these conditions, the transitions between open and first blocked states are indeed too fast to be resolved with single-channel recordings. On the other hand, during a macroscopic current transient elicited by a large positive voltage step, the second blocked state (strongly favored by positive potentials; Fig. 10) becomes populated and, consequently, a low concentration of spermine suffices to produce measurable channel block. Since channel block effectively occurs as soon as the blocker enters the inner pore and before it reaches its final destination, blocking rate is limited by the pseudo-first-order rate constant k_1[spermine]. At appropriately low spermine concentrations, k_1 can be determined.

A pertinent question is whether the (admittedly low) permeation rate of spermine through IRK1 confounds our analysis of spermine block and/or complicates comparison with that of bis-QA_{C10} block. We recall that spermine exists (Fig. 11) in different protonated states near neutral pH. In the more (perhaps fully) protonated form, spermine inhibits IRK1 with higher affinity and has a finite probability of traversing the selectivity

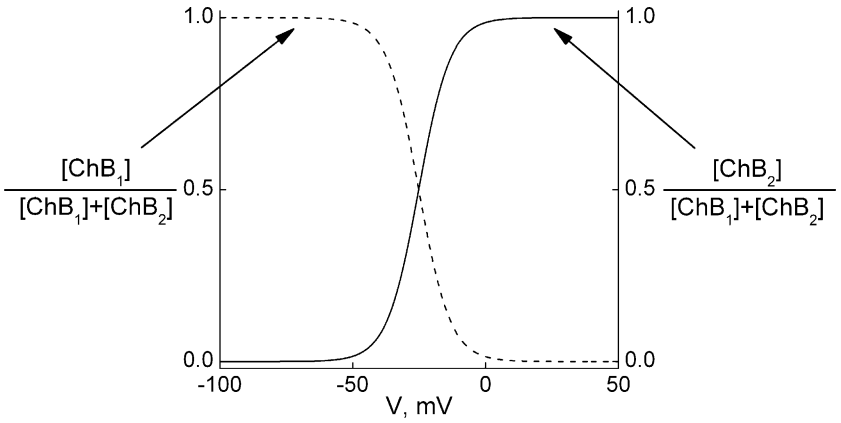

FIGURE 10. Distribution of the two blocked states of the model in Fig. 9 as a function of voltage. The relative distributions of the first (dashed curve) and second (solid curve) blocked states, computed using Eq. 2 and the parameters K_2 ($=[ChB_1]/[ChB_2]$) = 1.44×10^{-2} and $Z_2 = 4.23$ obtained from a fit of Eq. 1 to the data of Fig. 6 B, are plotted against membrane voltage.

filter (Guo and Lu, 2000a). Previous studies estimated the ratio of the rates of spermine punchthrough versus return to the intracellular solution as 2×10^{-2} (Guo and Lu, 2000a). Given the value of $\sim$500 s^{-1} obtained above for $^{app}k_{off}$ (Fig. 8 B and Fig. 9), we can now estimate the spermine punchthrough rate as $\sim$10 s^{-1}, at least 10^5-fold slower than K^+ permeation. Any current carried by spermine itself would be difficult to measure experimentally. The residual ("offset") current at positive potentials, which causes a plot of relative conductance against voltage in the presence of spermine to deviate from a Boltzmann function (see Fig. 3 of Guo and Lu, 2003; cf. Fig. 3 of Kurata et al., 2004) is carried by K^+ ions during the interval between a spermine molecule punching through the ion selectivity filter and reblock by the next spermine entering the inner pore. The deviation becomes less pronounced at high spermine concentrations (see Fig. 3 of Guo and Lu, 2003) because the (re)blocking rate (k_1[spermine]) is high, which shortens the interval of restored K^+ flux. At sufficiently high concentrations of spermine, the deviation from a pure Boltzmann function practically vanishes so that the parameters obtained from a fit of Eq. 1 (without allowance for spermine permeation) numerically approximate the equilibrium parameters determined from a fit of data obtained at low spermine concentrations with an equation that does allow for blocker permeation (Guo and Lu, 2000a). We find this is the case at 100 μM spermine because K_1K_2 determined from the data obtained at that relatively high concentration (Fig. 6 B) and the overall equilibrium constant determined at much lower concentrations (but with allowance for spermine punchthrough; e.g., Guo and Lu, 2003) are both about micromolar with a valence of $\sim$5.

For a valence of 5 to result from K^+ ions traversing the electric field requires only that five K^+ ions be displaced across the K^+ selectivity filter, with inability to bypass the blocker and "leak" back to the cytoplasm. The K^+ ions themselves may readily mix in the inner pore, i.e., there is no requirement for single filing. If any leakage does occur, then more K^+ ions must be present in the inner pore to produce the same valence. The value of the Ussing flux ratio exponent (n' = 2.2) determined by Stampe et al. (1998) in IRK1 is a lower-limit estimate of the number of K^+ ions subject to single filing, not the total number of K^+ ions in the pore. In light of the fact that the apparent valence of channel block by linear diamines rises from $\sim$2 to $\sim$5 as the alkyl chain is lengthened by five methylene groups (Fig. 6 B of Guo et al., 2003), part of the overall valence ($\sim$5) associated with the binding of spermine in the cavity may reflect the net movement of K^+ ions within (e.g., cartoon in Fig. 4 of Guo et al., 2003), or perhaps out of, the selectivity filter. Even if the net distribution of K^+ ions within the selectivity filter remained unaffected by the presence of a blocker molecule in the cavity, the inner pore would have to accommodate no

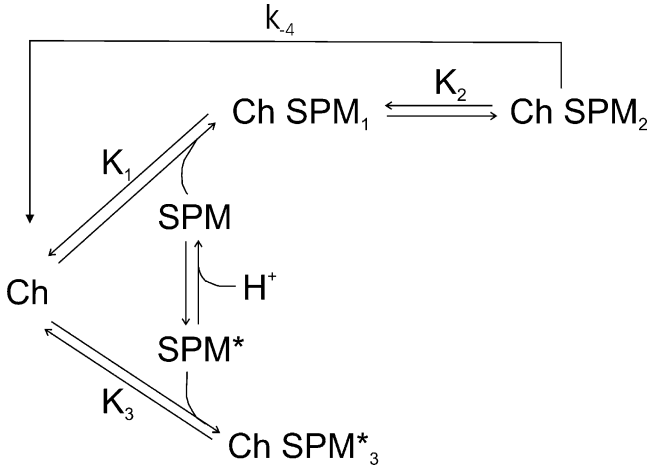

FIGURE 11. Expanded version of model in Fig. 9 where the blocker spermine exists in two protonation forms. In the more protonated (more charged) form spermine (SPM) traverses the pore at a low rate ($k_{-4} \sim 10\ s^{-1}$). K_3 ($\sim 10^{-5}$ M) is the equilibrium dissociation constant for binding of the less protonated (non or much less permeating) form of spermine (SPM*) to the channel (K^b_1 in Guo and Lu, 2000b). Values of rate constants and valences for other transitions are as in Fig. 9.

more than five K^+ ions, a not unrealistic requirement given its 50–70-Å length (Nishida and MacKinnon, 2002; Kuo et al., 2003).

We now examine a recent study of diamine block of wild-type and mutant Kir6.2 channels, which was interpreted to support a model of steeply rectifying Kir channels in which polyamines bind within the K^+ selectivity filter to produce strong voltage dependence (Kurata et al., 2004). The quoted authors examined how an acidic residue at various positions in and around the M2-lined "cavity" affects Kir6.2 inhibition by linear diamines (bis-alkylamines) of varying length, and analyzed the data with thermodynamic cycles. Although experiments and analyses in their study of Kir6.2 resemble those of Guo et al. (2003) and Guo and Lu (2003) on IRK1, the results and conclusions differ greatly. In the latter studies of IRK1, the coupling coefficient Ω (Hidalgo and MacKinnon, 1995) between diamines and D172 rises sharply for alkyl chain lengths beyond C6, peaks at C9 ($RT\ln \Omega \approx 1.5$ kcal/mole), and drops again for longer chains. The rise of the Ω value with alkyl chain length suggests a model in which the leading amine of long chains extends further outwardly into the "cavity" where D172 is located, and the dropoff reflects the leading amine overshooting D172 (and/or the chain buckling). In the study of Kir6.2 by Kurata et al. (2004), the findings are complex and there is no peak in the relation between Ω and alkyl chain length. We argue below that the discrepancy reflects critical differences in blocking properties between the two channels, and possibly also in the method of obtaining the constants used to compute Ω.

Thermodynamic mutant cycle analysis is typically performed to determine the interaction energy between two given elements of a protein, or of a protein–protein or ligand–receptor complex (Carter et al., 1984; Horovitz and Fersht, 1990; Schreiber and Fersht, 1995) and/or to infer their physical proximity (Hidalgo and MacKinnon, 1995; Ranganathan et al., 1996). The elements of interest are usually two amino acid residues or, as here, a given residue versus the difference between two amine blockers. If two elements are energetically coupled, then the magnitude of the free energy change ($RT\ln \Omega$) caused by modifying (in the case of residues, mutating) one element should depend on whether the other is modified or not. Valid analysis requires that the modification (mutation) not significantly alter the structure of the complex beyond the modified element (replaced side chain) or, in the present case, not alter the physical location of the blocker in the pore. To satisfy that prerequisite, multiple high-affinity interactions between blocker and channel must exist so that the blocker remains at the same locus with or without the mutation. In general, only a "unique" (or in some cases a couple of) nonunity Ω can safely be taken as indicating energetic coupling between the tested elements, because a mutation-induced distortion of the blocker-channel spatial arrangement would generate significant nonunity Ω values for many or all residues when tested against many or all blockers.

IRK1 (the channel studied by Guo et al., 2003 and Guo and Lu, 2003) binds linear diamines with high affinity, and the D172N mutation in M2 causes only a modest (<2 kcal/mole) lowering of interaction energy, and a small drop in apparent valence that can be ascribed to reduced K^+ occupancy of the D172N mutant channel's inner pore. Thus, the mutation does not appear to significantly alter the blocker position in the pore, as required for proper application of mutant cycle analysis. Much or most of the interaction energy of these diamines is clearly unrelated to D172 and probably reflects hydrophobic interactions, especially for long ones. On the other hand, Kir6.2 (the channel studied by Kurata et al., 2004) binds these amine blockers with very low (millimolar) affinity, and substituting an acidic residue at many sites in M2 dramatically increases both the apparent affinity and the valence of channel block. As Kurata et al. (2004) point out, the mutation-induced boost in apparent valence is too great to be ascribed to an increased presence of K^+ ions in the pore. It must, instead, reflect the fact that the mutation causes blockers to bind at a deeper location. That is, the mutation alters the spatial relation between blocker and pore, precluding a simple physical interpretation of the mutant cycle data. The computed Ω value now reflects not only the interaction between a given blocker–residue pair but also the energy difference between shallow and deep bound states. It is for this reason that our group chose to perform the thermodynamic cycle analysis on high-affinity IRK1, even though low-affinity ROMK1 (Kir1.1) was better understood and offers many technical advantages (e.g., Lu and MacKinnon, 1994). A second complicating factor in the analysis by Kurata et al. (2004) is the following. The coupling coefficient Ω is a measure of relative binding energies and must therefore be computed from equilibrium constants. Kurata et al. (2004) computed Ω from empirical steady-state constants ($K_{1/2}$) obtained by fitting the normalized G–V curves (in the presence of a single blocker concentration) with a modified Boltzmann function. The modified function included an undefined offset constant to account for a varying residual (up to 25% of maximum) K^+ current at positive voltages, probably resulting from blocker punchthrough. Absent information on how each nonequilibrium $K_{1/2}$ value differs from a true equilibrium dissociation constant, and on whether it reflects the properties of a well-defined blocked state rather than a mixture of states, Ω computed in this fashion will remain difficult to interpret.

In summary, we show that bis-QA_{C10}, at nearly the same length as spermine but with much wider head groups, blocks IRK1 channels with about the same overall voltage dependence as spermine does. Since the ~6-Å-wide head group of bis-QA_{C10} is unlikely to penetrate deep into the ~3-Å-wide K^+ selectivity filter, this observation lends strong and independent support to the hypothesis that the voltage dependence of IRK1 block by spermine results primarily from K^+ ions, not spermine itself, traversing the transmembrane electrical field that drops mainly across the narrow selectivity filter. We emphasize that even though the general features of the blocker-K^+ displacement model for inward rectification in IRK1 channels most probably apply to other Kir channels, caution must be exercised when specific details are considered, such as the number of experimentally identifiable blocked states, relations between a given set of blockers and certain channel residues, the impact of mutations at certain positions on the interactions of permeant or blocking ions with the pore, etc. This is because, among various homologous Kir channels, the side-chain nature and packing of many residues around the pore differ so that, for a given blocker, the overall binding energy is distributed differently over various participating channel residues.

We thank L.Y. Jan (University of California, San Francisco, CA) for the IRK1 channel cDNA clone, J. Yang (Columbia University, New York, NY) for the cDNA subcloned in the pGEM-HESS vector, and P. De Weer for critical review and discussion of our manuscript.

This study was supported by National Institutes of Health grant GM55560. H.-G. Shin was the recipient of a post-doctoral fellowship from Pennsylvania-Delaware Affiliate of the American Heart Association.

Olaf S. Andersen served as editor.

Submitted: 20 December 2004
Accepted: 23 February 2005

REFERENCES

Armstrong, C.M., and L. Binstock. 1965. Anomalous rectification in the squid giant axon injected with tetraethylammonium chloride. *J. Gen. Physiol.* 48:859–872.

Ashcroft, F.M. 2000. Ion Channels and Disease: Channelopathies. Academic Press, San Diego. 481 pp.

Carter, P.J., G. Winter, A.J. Wilkinson, and A.R. Fersht. 1984. The use of double mutants to detect structural changes in the active site of the tyrosyl-tRNA synthetase (*Bacillus stearothermophilus*). *Cell.* 38:835–840.

Dibb, K.M., T. Rose, S.Y. Makary, T.W. Claydon, D. Enkvetchakul, R. Leach, C.G. Nichols, and M.R. Boyett. 2003. Molecular basis of ion selectivity, block, and rectification of the inward rectifier Kir3.1/Kir3.4 channel. *J. Biol. Chem.* 278:49537–49548.

Fakler, B., U. Brandle, E. Glowatzki, S. Weidemann, H.P. Zenner, and J.P. Ruppersberg. 1995. Strong voltage-dependent inward rectification of inward rectifier K^+ channels is caused by intracellular spermine. *Cell.* 80:149–154.

Ficker, E., M. Taglialatela, B.A. Wible, C.M. Henley, and A.M. Brown. 1994. Spermine and spermidine as gating molecules for inward rectifier K^+ channels. *Science.* 266:1068–1072.

Guo, D., and Z. Lu. 2000a. Mechanism of IRK1 channel block by intracellular polyamines. *J. Gen. Physiol.* 115:799–813.

Guo, D., and Z. Lu. 2000b. Pore block versus intrinsic gating in the mechanism of inward rectification in the strongly rectifying IRK1 channel. *J. Gen. Physiol.* 116:561–568.

Guo, D., and Z. Lu. 2001. Kinetics of inward-rectifier K^+ channel block by quaternary alkylammonium ions: dimension and properties of the inner pore. *J. Gen. Physiol.* 117:395–405.

Guo, D., and Z. Lu. 2002. IRK1 inward rectifier K^+ channels exhibit no intrinsic rectification. *J. Gen. Physiol.* 120:539–551.

Guo, D., and Z. Lu. 2003. Interaction mechanisms between polyamines and IRK1 inward rectifier K^+ channels. *J. Gen. Physiol.* 122:485–500.

Guo, D., Y. Ramu, A.M. Klem, and Z. Lu. 2003. Mechanism of rectification in inward-rectifier K^+ channels. *J. Gen. Physiol.* 121:261–275.

Hagiwara, S., S. Miyazaki, and N.P. Rosenthal. 1976. Potassium current and the effect of cesium on this current during anomalous rectification of the egg cell membrane of a starfish. *J. Gen. Physiol.* 67:621–638.

Hagiwara, S., and K. Takahashi. 1974. The anomalous rectification and cation selectivity of the membrane of a starfish egg cell. *J. Membr. Biol.* 18:61–80.

Hidalgo, P., and R. MacKinnon. 1995. Revealing the architecture of a K^+ channel pore through mutant cycles with a peptide inhibitor. *Science.* 268:307–310.

Hille, B. 2001. Ion Channels of Excitable Membranes. Third edition. Sinauer Associates, Inc., Sunderland, MA. 814 pp.

Hodgkin, A.L., and P. Horowicz. 1959. The influence of potassium and chloride ions on the membrane potential of single muscle fibres. *J. Physiol.* 148:127–160.

Horovitz, A., and A.R. Fersht. 1990. Strategy for analysing the cooperativity of intramolecular interactions in peptides and proteins. *J. Mol. Biol.* 214:613–617.

Huang, C.L., S. Feng, and D.W. Hilgemann. 1998. Direct activation of inward rectifier potassium channels by PIP_2 and its stabilization by $G_{\beta\gamma}$. *Nature.* 391:803–806.

John, S.A., L.-H. Xie, and J.N. Weiss. 2004. Mechanism of inward rectification in Kir channels. *J. Gen. Physiol.* 123:623–625.

Katz, B. 1949. Les constantes électriques de la membrane du muscle. *Arch. Sci. Physiol. (Paris).* 3:285–299.

Kubo, Y., and Y. Murata. 2001. Control of rectification and permeation by two distinct sites after the second transmembrane region in Kir2.1 K^+ channel. *J. Physiol.* 531:645–660.

Kubo, Y., T.J. Baldwin, Y.N. Jan, and L.Y. Jan. 1993. Primary structure and functional expression of a mouse inward rectifier potassium channel. *Nature.* 362:127–133.

Kuo, A., J.M. Gulbis, J.F. Antcliff, T. Rahman, E.D. Lowe, J. Zimmer, J. Cuthbertson, F.M. Ashcroft, T. Ezaki, and D.A. Doyle. 2003. Crystal structure of the potassium channel KirBac1.1 in the closed state. *Science.* 300:1922–1926.

Kurata, H.T., L.R. Philips, T. Rose, G. Loussouarn, S. Herlitze, H. Fritzenschaft, D. Enkvetchakul, C.G. Nichols, and T. Baukrowitz. 2004. Molecular basis of inward rectification: polyamine interaction sites located by combined channel and ligand mutagenesis. *Journal of General Physiology.* 124:541–554.

Liman, E.R., J. Tytgat, and P. Hess. 1992. Subunit stoichiometry of a mammalian K^+ channel determined by construction of multimeric cDNAs. *Neuron.* 9:861–871.

Lopatin, A.N., E.N. Makhina, and C.G. Nichols. 1994. Potassium channel block by cytoplasmic polyamines as the mechanism of intrinsic rectification. *Nature.* 372:366–369.

Lopatin, A.N., E.N. Makhina, and C.G. Nichols. 1995. The mechanism of inward rectification of potassium channels: "long-pore

plugging" by cytoplasmic polyamines. *J. Gen. Physiol.* 106:923–955.

Lu, Z. 2004. Mechanism of rectification in inward-rectifier K^+ channels. *Annu. Rev. Physiol.* 66:103–129.

Lu, Z., and R. MacKinnon. 1994. Electrostatic tuning of Mg^{2+} affinity in an inward-rectifier K^+ channel. *Nature.* 371:243–246.

Matsuda, H., A. Saigusa, and H. Irisawa. 1987. Ohmic conductance through the inwardly rectifying K^+ channel and blocking by internal Mg^{2+}. *Nature.* 325:156–159.

Miller, C. 1982. Bis-quaternary ammonium blockers as structural probes of the sarcoplasmic reticulum K^+ channel. *J. Gen. Physiol.* 79:869–891.

Nishida, M., and R. MacKinnon. 2002. Structural basis of inward rectification: cytoplasmic pore of the G protein-gated inward rectifier GIRK1 at 1.8-Å resolution. *Cell.* 111:957–965.

Noble, D. 1962. A modification of Hodgkin-Huxley equations applicable to Purkinje fibre action and pace-maker potentials. *J. Physiol.* 160:317–352.

Noble, D. 1965. Electrical properties of cardiac muscle attributable to inward going (anomalous) rectification. *Journal of Cellular and Comparative Physiology.* 66(3P2S):127–136.

Ranganathan, R., J.H. Lewis, and R. MacKinnon. 1996. Spatial localization of the K^+ channel selectivity filter by mutant cycle-based structure analysis. *Neuron.* 16:131–139.

Schreiber, G., and A.R. Fersht. 1995. Energetics of protein-protein interactions: analysis of the barnase-barstar interface by single mutations and double mutant cycles. *J. Mol. Biol.* 248:478–486.

Stampe, P., J. Arreola, P. Perez-Cornejo, and T. Begenisich. 1998. Nonindependent K^+ movement through the pore in IRK1 potassium channels. *J. Gen. Physiol.* 112:475–484.

Stanfield, P.R., N.W. Davies, P.A. Shelton, M.J. Sutcliffe, I.A. Khan, W.J. Brammar, N.B. Standen, and E.C. Conley. 1994. A single aspartate residue is involved in both intrinsic gating and blockage by Mg^{2+} of the inward rectifier, IRK1. *J. Physiol.* 478:1–6.

Stanfield, P.R., S. Nakajima, and Y. Nakajima. 2002. Constitutively active and G-protein coupled inward rectifier K^+ channels: Kir2.0 and Kir3.0. *Rev. Physiol. Biochem. Pharmacol.* 145:47–179.

Taglialatela, M., E. Ficker, B.A. Wible, and A.M. Brown. 1995. C-terminus determinants for Mg^{2+} and polyamine block of the inward rectifier K^+ channel IRK1. *EMBO J.* 14:5532–5541.

Taglialatela, M., B.A. Wible, R. Caporaso, and A.M. Brown. 1994. Specification of pore properties by the carboxyl terminus of inwardly rectifying K^+ channels. *Science.* 264:844–847.

Vandenberg, C.A. 1987. Inward rectification of a potassium channel in cardiac ventricular cells depends on internal magnesium ions. *Proc. Natl. Acad. Sci. USA.* 84:2560–2564.

Wible, B.A., M. Taglialatela, E. Ficker, and A.M. Brown. 1994. Gating of inwardly rectifying K^+ channels localized to a single negatively charged residue. *Nature.* 371:246–249.

Xie, L.-H., S.A. John, and J.N. Weiss. 2002. Spermine block of the strong inward rectifier potassium channel Kir2.1: dual roles of surface screening and pore block. *J. Gen. Physiol.* 120:53–66.

Xie, L.-H., S.A. John, and J.N. Weiss. 2003. Inward rectification by polyamines in mouse Kir2.1 channels: synergy between blocking components. *J. Physiol.* 550:67–82.

Yang, J., Y.N. Jan, and L.Y. Jan. 1995. Control of rectification and permeation by residues in two distinct domains in an inward rectifier K^+ channel. *Neuron.* 14:1047–1054.